Finite Element Solver for Thermo-Hydraulic Optimization of Architected Ceramics (NExT I-Site industrial partnership program: OPTHOCERA): project overview

Benoit Rousseau, Salih Ouchtout, Jérôme Delmas, Christophe Le Bozec, Gwenael Biotteau, Steven Le Corre, Jerôme Vicente, Ludovic Charpentier, Cindy Schick, Eric Louradour, et al.

Finite Element Solver for Thermo-Hydraulic Optimization of Architected Ceramics (NExT I-Site industrial partnership program: OPTHOCERA): project overview

Benoit Rousseau[1], Salih Ouchtout[1], Jerôme Delmas[1], Christophe le Bozec[1], Gwenaell Biotteau[1], Steven Le Corre[1], Jerôme Vicente[2], Ludovic Charpentier[3], Cindy Schick[4], Eric Louradour[4], Christophe Chaput[4]

[1] Nantes Université, CNRS, Nantes, France, [2] AMU Université, CNRS, Marseilles, France, [3] CNRS, Font-Romeu, France, [4] 3D CERAM SINTO Bonnac La Côte, France

September 27-30, 2022
Albuquerque, NM, USA
28th SolarPACES Conference

Decarbonization of high-temperature industrial processes (T> 1,000°C)

- Stabilization of global warming[1)]→net-zero emission of CO_2 in human activities (industry, transpoirt, residential sector…)
- Industry accounts for 32 % of the final energy consumption with 74 % of this component is required for heat production of which 90 % is provided by burning fossil combustible (coal, oil, gas)
- 48 % of energy consumption for producing industrial heat is due to high-temperature processes (T > 400°C)

Production of fuels and chemical commodities

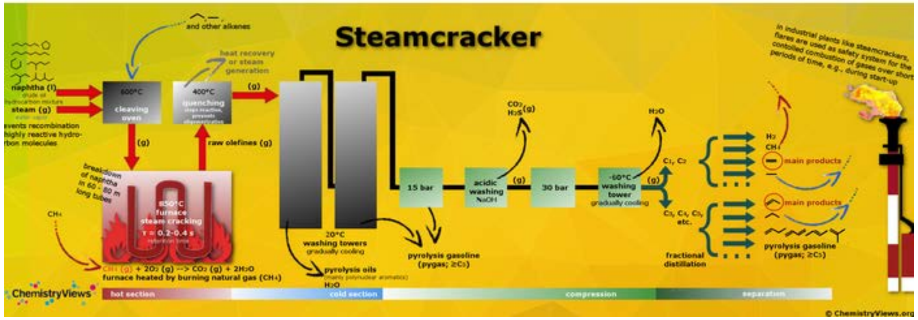

Zimmermann in *Ullmann's Encyclopedia of Industrial Chemistry*, Wiley-VCH, Weinheim, Germany, **2009**

Mineral sector

Metallurgical sector

[1)] Masson-Delmotte et al., In: Climate Change 2021 Contribution of Working Group I to the Sixth Assessment Report of the Intergovernmental Panel on Climate Change.

Interest of high-temperature concentrated solar heat

- Solar energy →abundant : 1% of the 3.8×10^{24} joules of solar energy reaching the earth's surface every year → 40 times the electricity generated globally
- But dilute, geographically non uniform, temporally intermittent, variable

- Concentration[2)] of solar radiation (paraboloid dishes and solar towers) →1,000°C (with incident fluxes > $1 MW/m^2$)

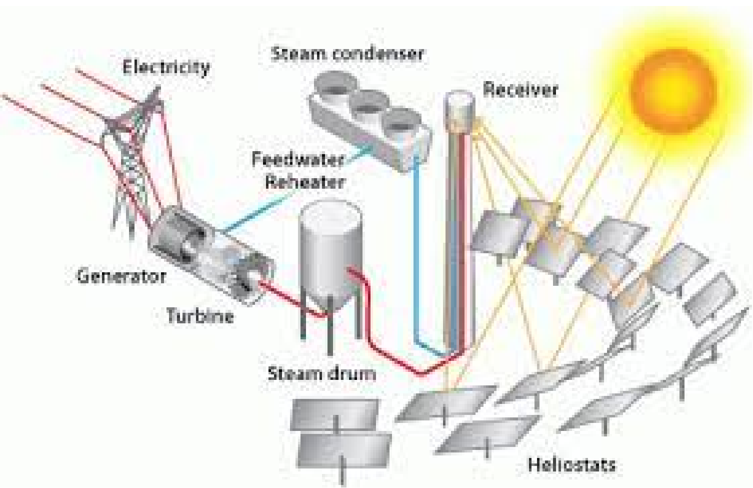

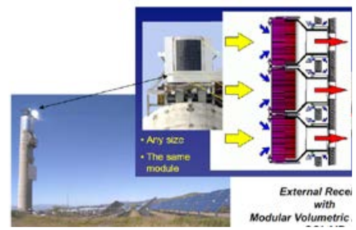

SOLAIR program, Julich, Germany

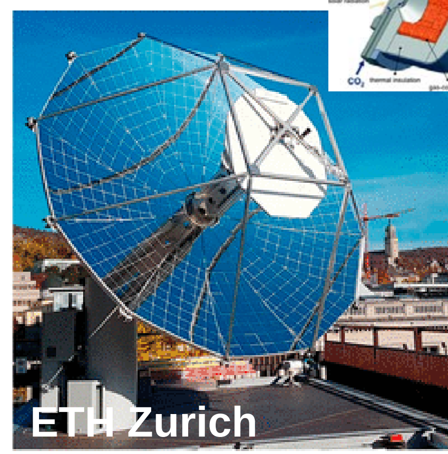

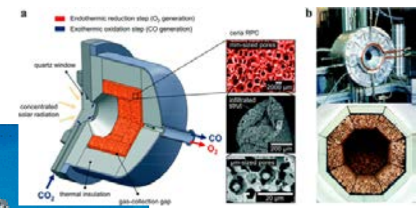

Syngas production, Zurich, Switzerland

- Development of **high-temperature solar receivers with high solar-to-heat conversion efficiency and service life of 10,000 cycles under harsh conditions** → thermal, mechanical, material challenges

[2)] Romero, M., Steinfeld, A., 2012. Concentrating solar thermal power and thermochemical fuels. Energy Environ. Sci. 5, 9234–9245

Volumetric solar receivers = radiative-convective heat exchangers

Principle

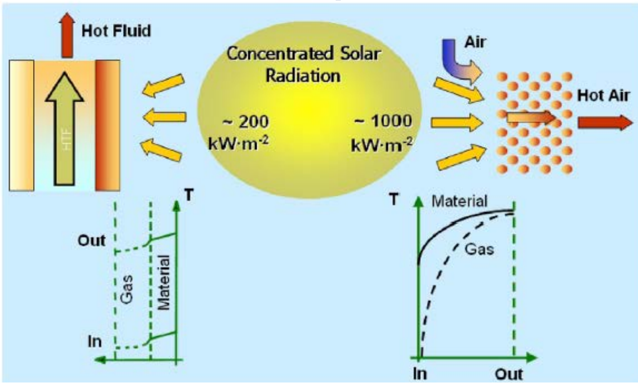

Avila-Marin et *al.*, Renewable and Sustainable Energy Reviews, 2019, 111 15

Conventional 3D geometries

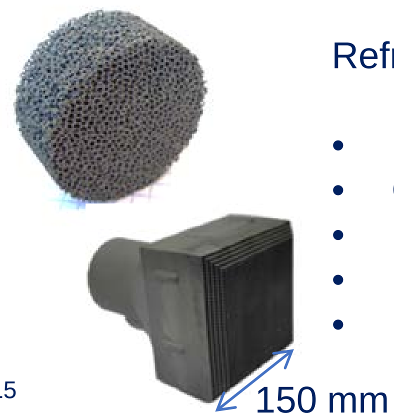

Refractory porous ceramics (SiC, Al_2O_3,…)

- High solar absorptance
- Good thermal conductivity
- High volumetric surface
- Low thermal emittance
- High thermal shock resistance

New concepts based on additive manufacturing coupled with radiative transfer design

→ Improvement of the volume propagation of concentrated solar light, reduction of thermal emission

Luque et *al.*, Solar Energy, 2018, 174, 342

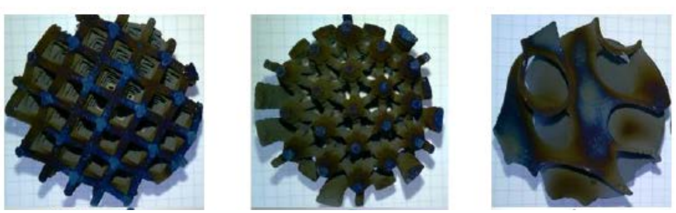

Heisel et *al.*, Solar Energy Materials and Solar cells, 2021, 231, 111336

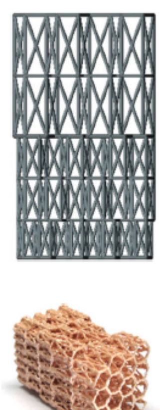

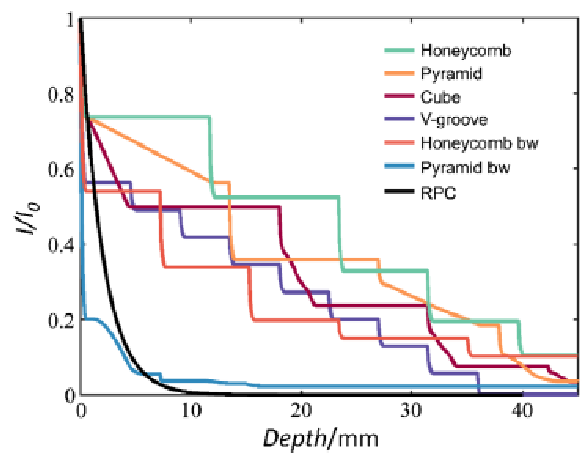

Hoes et *al.*, Energy Technol. 2019, 7, 1900484

Numerical design approach coupled with additive manufacturing

Numerical design of 3D digitalized porous architectures (regular, pore size gradient)

Thermo-fluidic modelling→Temperature and flux fields (**HEM** or **DS**) (conduction, convection, radiation)

Optimization loop/textural constraints (solar-to heat efficiency, temperature profiles)

Optimized architectures → elaboration with additive manufacturing (stereolithography, binder jetting)

Performance tests : solar-to-heat conversion (OPTISOL bench, PROMES Odeillo, FRance).

cea irCer institut de recherche sur les céramiques LCTS

3DCERAM into Global Advanced Ceramics

Tamarys TAMARYS network

HEM : Homogeneous Equivalent Method → continuous scale approach
DS : Detailed Simulation → pore scale approach

OPTHOCERA program (1 year)

iusti UMR 7343 — LTEN UMR 6607 Laboratoire de Thermique et Énergie de Nantes

Numerical design of 3D digitalized porous architectures (regular, pore size gradient)

→

LTEN UMR 6607 Laboratoire de Thermique et Énergie de Nantes

Conductive-radiative modelling→Temperature and flux fields (HEM and DS)

↓

Selected architectures according to Planck number → elaboration by stereolithography

sinto 3DCERAM Global Advanced Ceramics

→

Performance tests : solar-to-heat conversion (OPTISOL bench, PROMES Odeillo, France).

PROMES

Radiative Transfer Equation : modelling of volume propagation of thermal and solar radiations

- Macro-porous ceramics $\rightarrow$ semi-transparent media (absorption, scattering, emission)
- Valid if the medium is homogeneous, continous and weakly spatially correlated

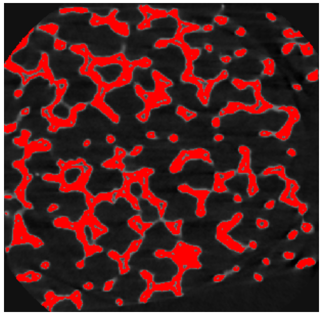

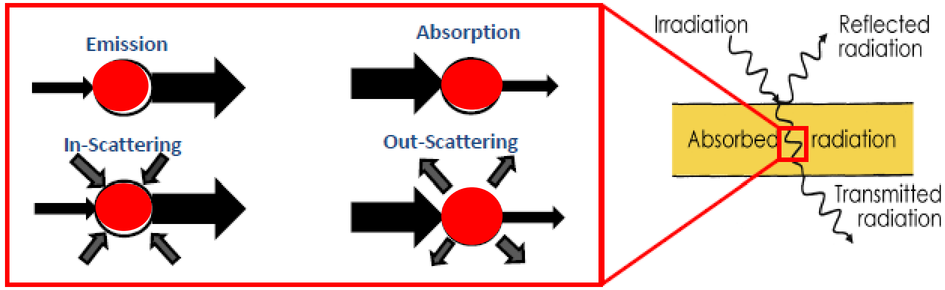

$$\hat{\Omega}.\nabla I_{\nu}(s,\hat{\Omega})+(\kappa_a+\kappa_s)\text{-}\kappa_s\int_{4\pi} I_{\nu}(s,\hat{\Omega})P(\hat{\Omega}'\rightarrow\hat{\Omega})d\hat{\Omega}'-\kappa_a I_{P\nu}=0$$

$$\nabla.\dot{q}''(s)=\int_0^{\infty}\kappa_{a\nu}4\pi I_{b\nu}(T)d\nu-\int_0^{\infty}\int_{4\pi}\kappa_{a\nu}I_{\nu}(s,\hat{\Omega})d\Omega d\nu$$

$$\rho c_p\frac{\partial T}{\partial t}(s)=\nabla.\left(k_{cond}\nabla T(s)-\dot{q}''(s)\right)$$

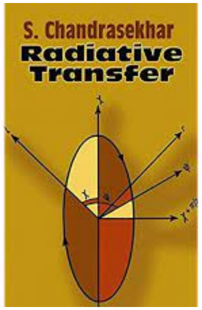

Chandrasekhar, Radiative Transfer, Dover, 1960

Methods for solving the steady-state RTE

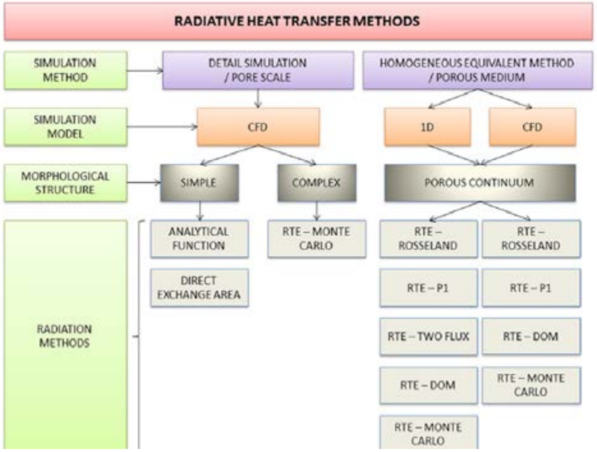

Avila-Marin et *al.*, Renewable and Sustainable Energy Reviews, 2019, 111 15

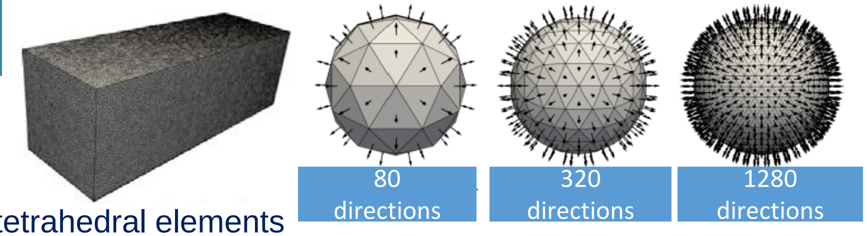

~10^7 tetrahedral elements

Fast, robust, accurate parallelized vectorial FEM solver

Badri et *al.*, Journal of Computational Physics, 2018, 360, 74-92

Badri et al. Journal of Quantitative Spectroscopy and Radiative Transfer 212 (2018): 59-74

Detailed Simulation (DS)

(discrete scale model)

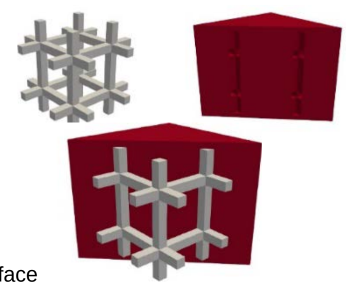

solid interface

$$\varepsilon n^2\sigma_B\left(T^{\partial}_{S-V}\right)^4 - \varepsilon\int_{\hat{\Omega}.n_s>0} I\left|\hat{\Omega}.n_s\right|d\hat{\Omega} = 0$$

fluid phase

$$\hat{\Omega}.\nabla I(s,\hat{\Omega}) = 0$$

Rosseland model

$$\nabla.\left(\frac{16n^2\sigma_B}{3(\kappa_a+\kappa_s)}T^3\nabla T\right) = \nabla.k_R\nabla T$$

Homogeneous Equivalent Model (HEM)

(continous scale model)

$$\hat{\Omega}.\nabla I(s,\hat{\Omega}) + (\kappa_a+\kappa_s) - \kappa_s\int_{4\pi} I(s,\hat{\Omega})P(\hat{\Omega}'\rightarrow\hat{\Omega})d\hat{\Omega}' - \kappa_a\frac{1}{\pi}\sigma_B n^2 T^4 = 0$$

$$P(\hat{\Omega}'\rightarrow\hat{\Omega}) = \frac{1}{4\pi}\frac{1-g^2}{\left(1+g^2-\hat{\Omega}.\hat{\Omega}'\right)^{3/2}}$$

$$\kappa_e = \kappa_a+\kappa_s = 4.8\frac{(1-p)}{d_{nom}} \quad \text{with} \quad \kappa_a = \varepsilon\kappa_e \quad \text{and} \quad \omega = \frac{\kappa_s}{\kappa_s+\kappa_a}$$

Local radiative properties from the bulk

Effective radiative properties → porosity, nominal pore diameter and emissivity

Use of the FEM solver for analyzing the coupling between conduction and radiation within a 1D slab sandwiched by a hot and a cold wall

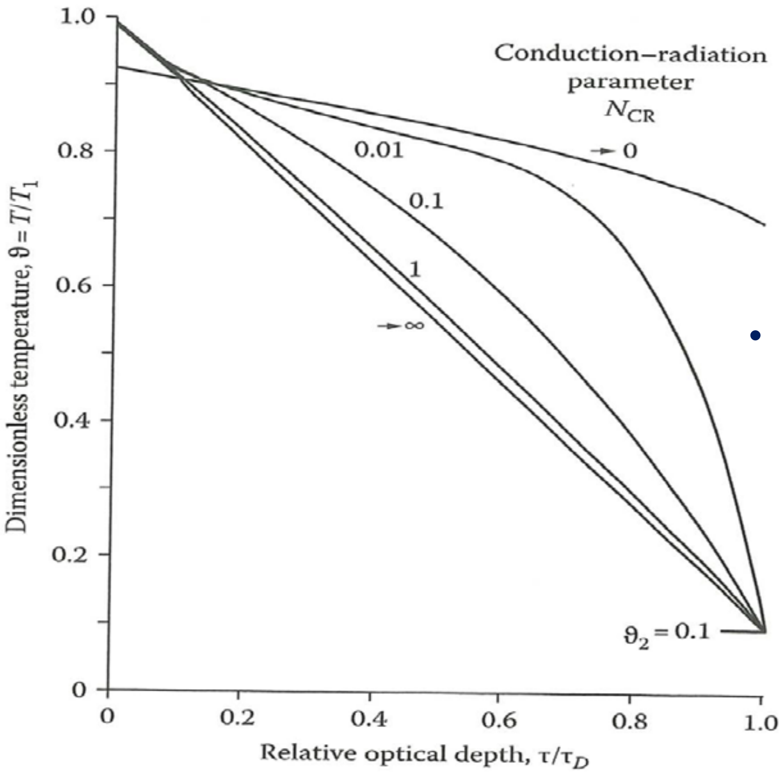

Viskanta & Grosh JHT (1962)

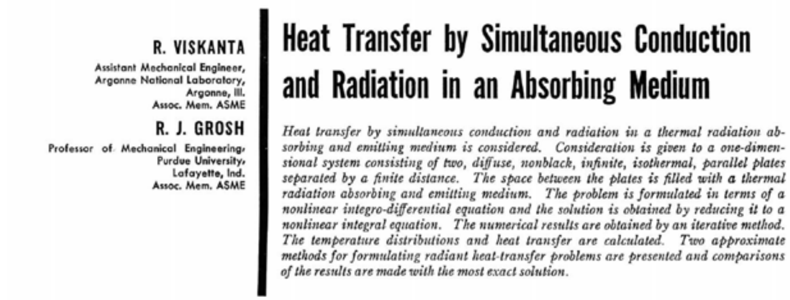

R. VISKANTA
Assistant Mechanical Engineer, Argonne National Laboratory, Argonne, Ill. Assoc. Mem. ASME

R. J. GROSH
Professor of Mechanical Engineering, Purdue University, Lafayette, Ind. Assoc. Mem. ASME

Heat Transfer by Simultaneous Conduction and Radiation in an Absorbing Medium

Heat transfer by simultaneous conduction and radiation in a thermal radiation absorbing and emitting medium is considered. Consideration is given to a one-dimensional system consisting of two, diffuse, nonblack, infinite, isothermal, parallel plates separated by a finite distance. The space between the plates is filled with a thermal radiation absorbing and emitting medium. The problem is formulated in terms of a nonlinear integro-differential equation and the solution is obtained by reducing it to a nonlinear integral equation. The numerical results are obtained by an iterative method. The temperature distributions and heat transfer are calculated. Two approximate methods for formulating radiant heat-transfer problems are presented and comparisons of the results are made with the most exact solution.

- 1D layer of translucent conducting-radiating medium between tow parallel black walls at temperature T_1 et T_2 with $\theta = T/T_1$ et $\theta_2 = T_2/T_1$

$$N = \frac{k_{cond}\kappa_a}{4\sigma_B T_1^3}$$ Planck or Stark number

$$N \to \infty$$ Pure conductive regime

$$N \to 0$$ Dominant radiative regime

For a porous ceramic with absorption and scattering phenomena

$$N = \frac{k_{cond}(\kappa_a + \kappa_s)}{4\sigma_B T_1^3}$$

Comparison between HEM model/exact solution from Viskanta

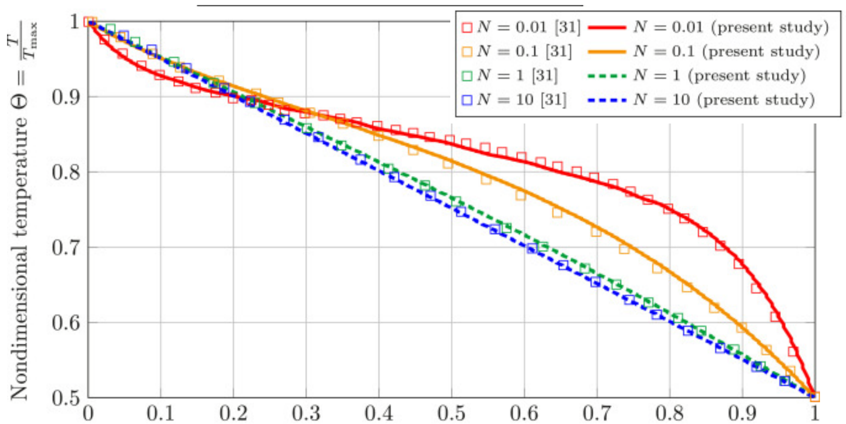

$\theta_2 = 0.5$; $T_1 = 2{,}222$ K, $T_2 = 1{,}111$ K, $\kappa_a = 2{,}625\ m^{-1}$, $\kappa_s = 0$

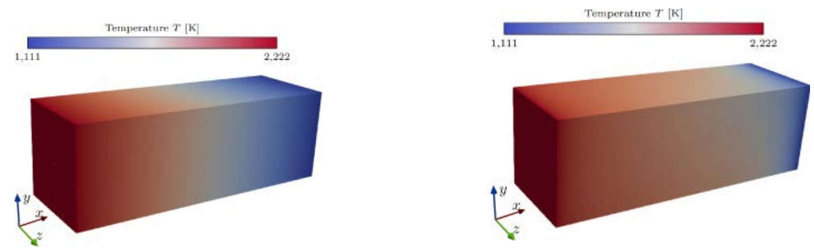

$N \to 0$

- Dominant radiative regime
- Increase of T near the cold wall
- $\tau = 0.9$ $(+36\ \%)$
- $\rightarrow$ @T=700 K , + 252 K
- low κ_e : for a given p, high d_{nom} (low PPI)

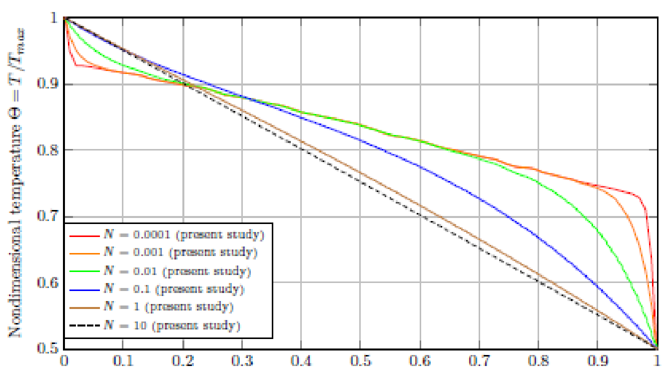

Typical values of N for real ceramic-based open cell foams (T=1,300 K)

material	Thermal conductivity @1000°C [W/(m.K)]	Porosity= 80 %, cell size = 2mm	Porosity=80 %, cell size = 4mm	Porosity= 80 %, cell size = 8mm	Porosity= 90 %, cell size = 2mm	Porosity= 90 %, cell size = 4mm	Porosity= 90 %, cell size = 8mm
alumina	~6.8	0,19652	0,09826	0,04913	0,09826	0,04913	0,02456
mullite	~3.2	0,09248	0,04624	0,02312	0,04624	0,02312	0,01156
cordierite	~1.5	0,04335	0,02167	0,01084	0,02167	0,01084	0,00542
silicon carbide	~50	1,44497	0,72249	0,36124	0,72249	0,36124	0,18062

Interest for semi-transparent porous ceramics with high p and high d_{nom}

Comparison of the Rosseland↔HEM model and of the HEM↔DS model

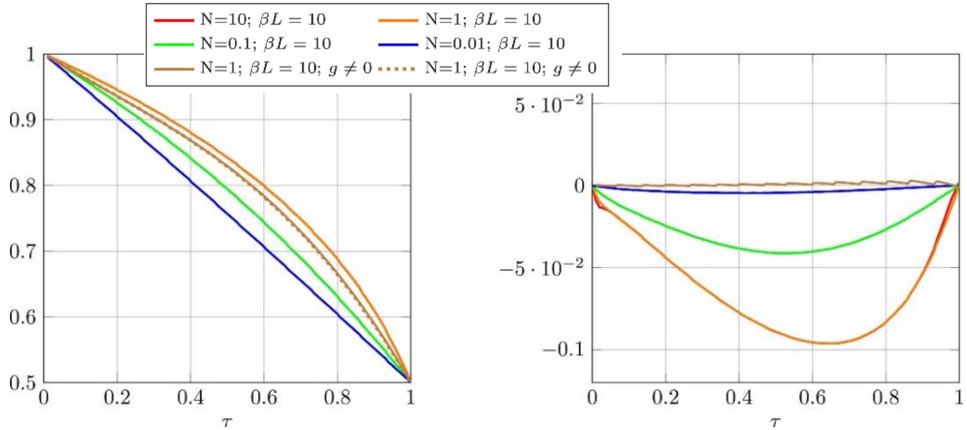

$$\hat{e}(u) = \frac{1}{L}\int_0^L u^2(x)dx$$

- Rosseland : less accurate model
- Up to 10 % of errors

θ_2= 0.5 ; T_1=2,222 K, T_1=1,111 K, κ_a = 26,250 m^{-1}, κ_s = 0

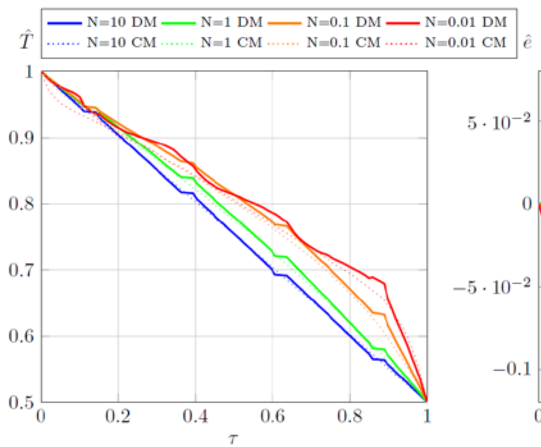

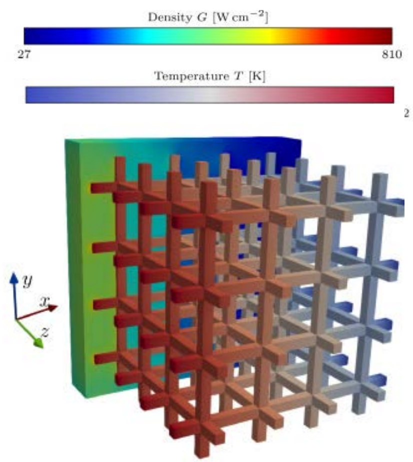

- HEM model :good approach for modelling thermal transfer and for performing future advanced (topology) optimisation process
- DS model : thermo-mechanical computation

	$N=10$			$N=1$			$N=0.1$			$N=0.01$		
Model Method	N-R	I F-P	F-P	N-R	I F-P	F-P	N-R	I F-P	F-P	N-R	I F-P	F-P
DS-CM	324 s	336 s	371 s	325 s	339 s	400 s	338	+∞	+∞	347	+∞	+∞
CS-CM	69 s	70 s	70 s	70 s	77 s	78 s	74 s	+∞	+∞	77 s	+∞	+∞
RM	9 s	–	10 s	10 s	–	13 s	11 s	–	17 s	11 s	–	+∞

331 860 tetrahedral elements for the solid phase and 1 753 680 elements for the fluid phase ; 62 processors, 128 directions

Thermal behaviour of 4 fictitious alumina-based Kelvin Cell Foams exposed to a collimated concentrated solar beam (10^6 W.m²)

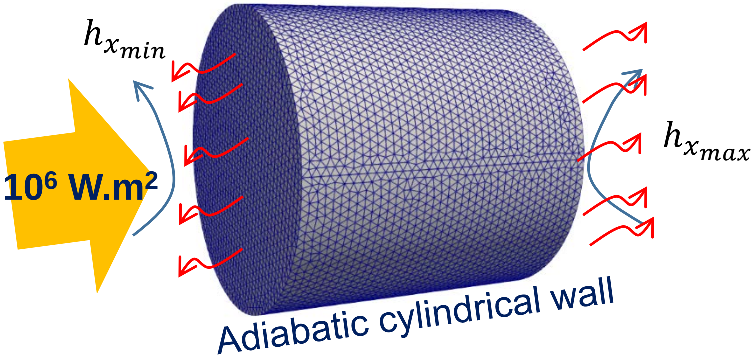

Case 1 d_{nom}=0,004 m

Case 2 d_{nom}=0,008 m

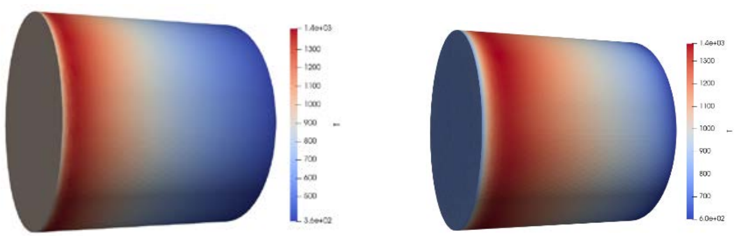

Case 3

Case 4

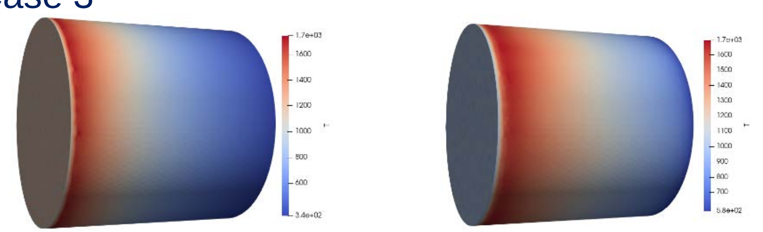

Porosity = 91 %, ∅ = 5 cm, h= 5 cm

	d_{nom}=0,004 m without coating Case 1	d_{nom}=0,008 m without coating Case 2	d_{nom}=0,004 m with coating Case 3	d_{nom}=0,008 m with coating Case 4
β_{eff}(m^{-1})	**108**	**54**	**108**	**54**
κ_{eff} (m^{-1})	33.7	12,7	79	33
σ_{eff} (m^{-1})	74.3	41.3	29	21
ε_{eff}	**0.31**	**0.24**	**0.73**	**0.61**
λ_{eff} (W.m^{-1}.K^{-1})	0,33	0,33	0,33	0,33
$N_{P,\beta_{eff}}$	**0,04422**	**0,02211**	**0,04422**	**0,02211**
ω_{eff}	**0.67**	**0.76**	**0.27**	**0.39**
ρ_{eff} (kg.m^3)	330	330	330	330
$C_{P,eff}$(J. Kg^{-1}K^{-1})	1200	1200	1200	1200
$h_{x_{min}} = 10h_{x_{max}}$ (W. m^{-2}.K^{-1})	10	10	10	10

Addition of an absorbing coating on the alumina ligaments

Thermal behaviour of porous alumina ceramics exposed to a collimated concentrated solar beam (10^6 W.m^2)

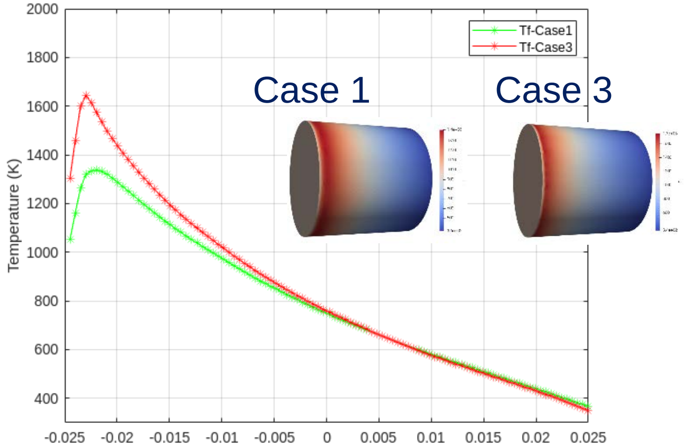

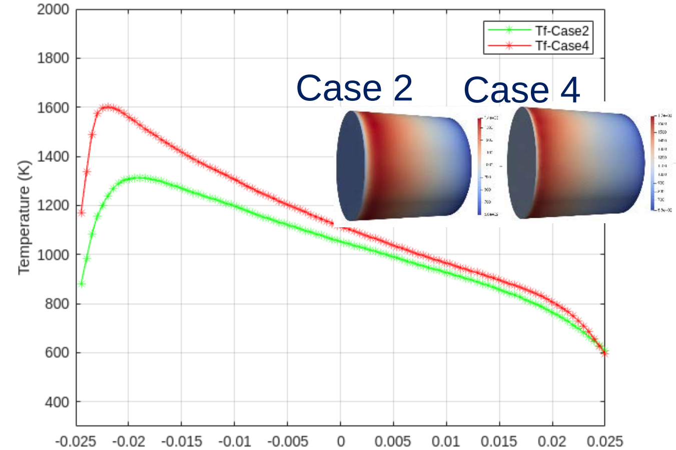

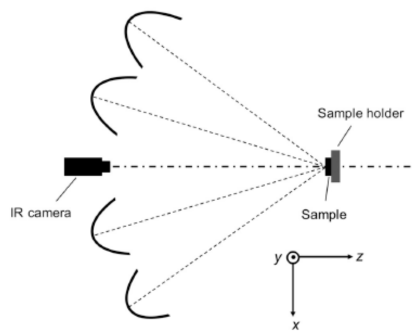

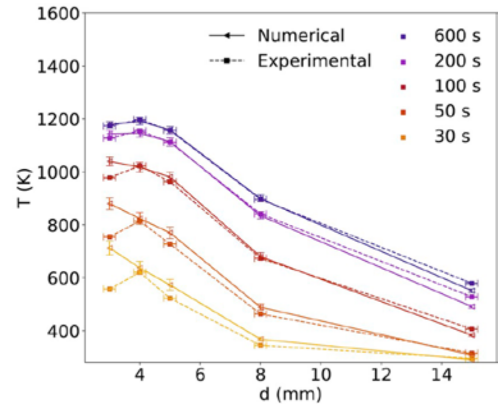

Similar temperature profile for alumina ceramics exposed to artificial concentrated solar flux.

Mora Monteros et *al.*, *Ceramics International 46 (2020) 2805–2815*

$N_{P,\beta_{eff}}(1,3) = 2N_{P,\beta_{eff}}(2,4) \rightarrow$ volume radiation effect more important

$\omega_{eff}(1,2) < \omega_{eff}(3,4) \rightarrow$ volume radiation effect more important

$\varepsilon_{eff}(1,2) < \varepsilon_{eff}(3,4) \rightarrow$ decreasing of the radiative losses at the front face

From the numerical design of porous ceramics up to elaboration thanks to stereolithography

genMat

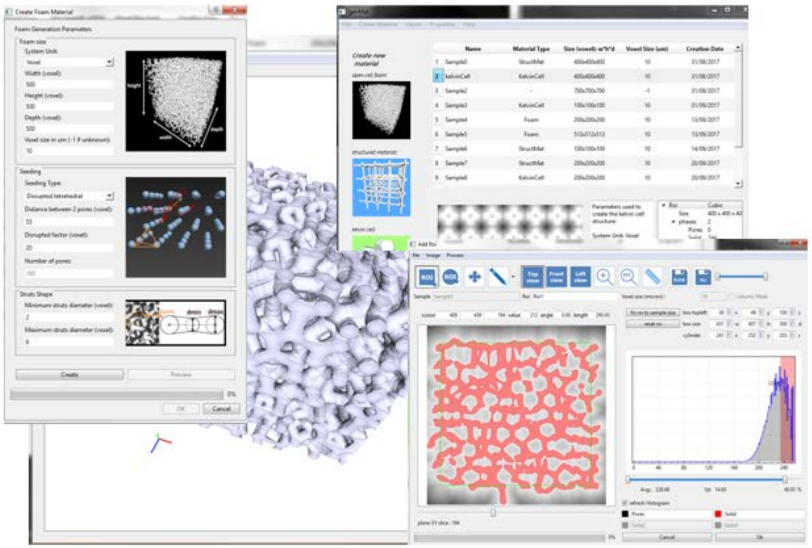

	Kelvin cell foam 1	Kelvin cell foam 2
d_{nom} (m)	0.004	0.008
p	91 %	91%
S_v (m^{-1})	704.288	314.751
h (m)	0.05	0.05
d (m)	0.05	0.05
β_{eff} (m^{-1})	**108**	**54**

Kelvin cell foam 1

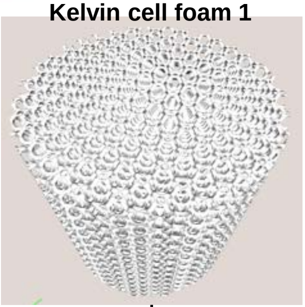

Kelvin cell foam 2

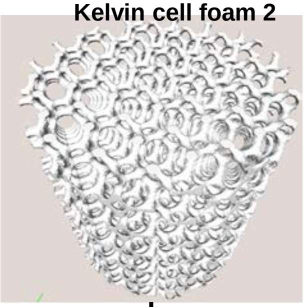

genMat→ stl files (100 Mo)→ SOLIDWORKS

3DCERAM sinto Global Advanced Ceramics

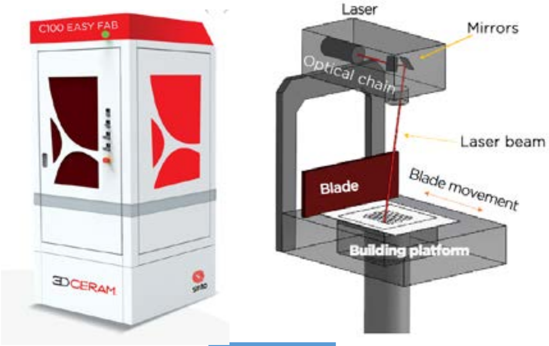

Densification control – sintering 1700°C smooth surface state

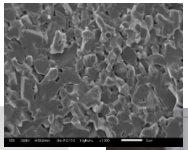

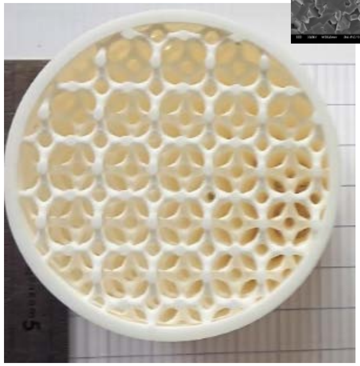

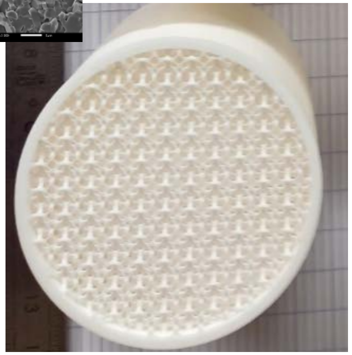

Improvement of the solar absorptance of the alumina skeleton with a commercial refractory black coating

spraying/drying in hood

heat treatment (900°C, 1h00)

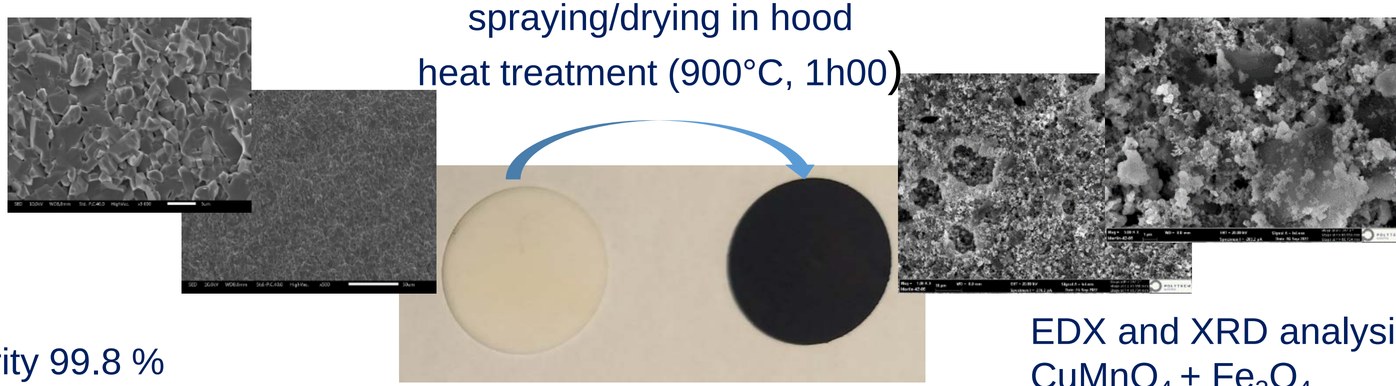

Al_2O_3 : purity 99.8 %

EDX and XRD analysis : $CuMnO_4 + Fe_3O_4$

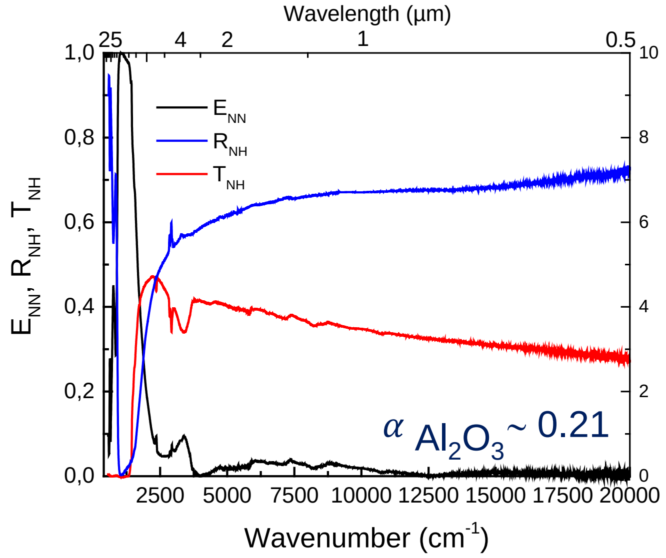

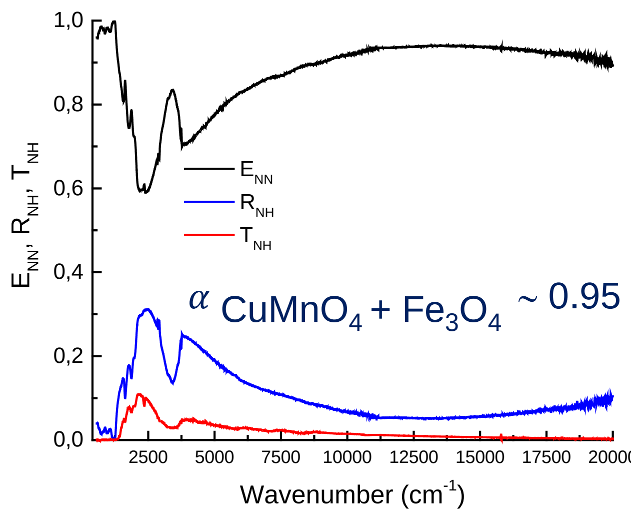

Numerical computations of the Kelvin cell foams emissivities with genMat

Parallelized Monte Carlo Ray-Tracing code

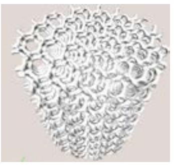

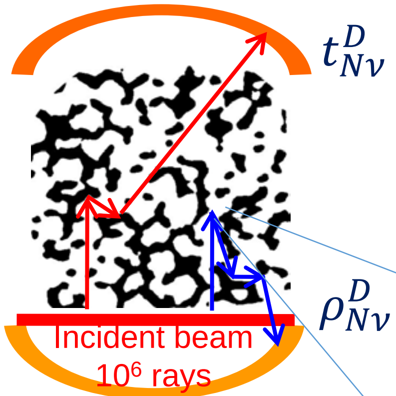

Macroscopic scale :
100,000 µm

Rousseau et al., JCPS, 2012

Guevelou et al., IJHMT 2016

Mesoscopic scale :
~100 µm

ρ Al_2O_3 ~ 0.79
ρ $CuMnO_4 + Fe_3O_4$ ~ 0.05

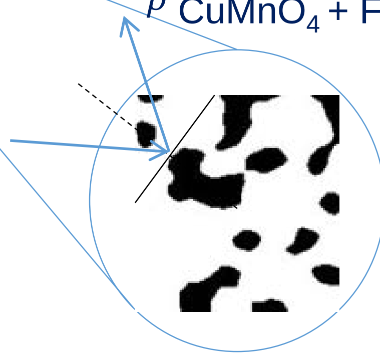

8 mm without coating
case 2

8 mm with coating
case 4

4 mm without coating
case 1

4 mm with coating
case 3

	d_{nom}=0,004 m without coating Case 1	d_{nom}=0,008 m without coating Case 2	d_{nom}=0,004 m with coating Case 3	d_{nom}=0,008 m with coating Case 4
ε_{eff}	**0.31**	**0.24**	**0.73**	**0.61**

Absorption length of the incident collimated beam : effect of d_{nom}

d_{nom}=0,004 m
with coating
case 3

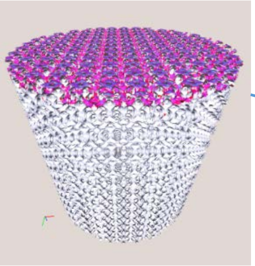

d_{nom}=0,004 m
without coating
case 1

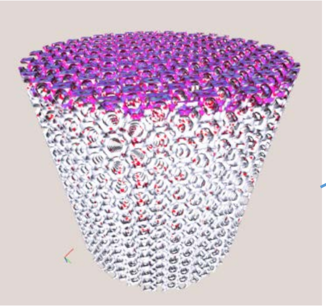

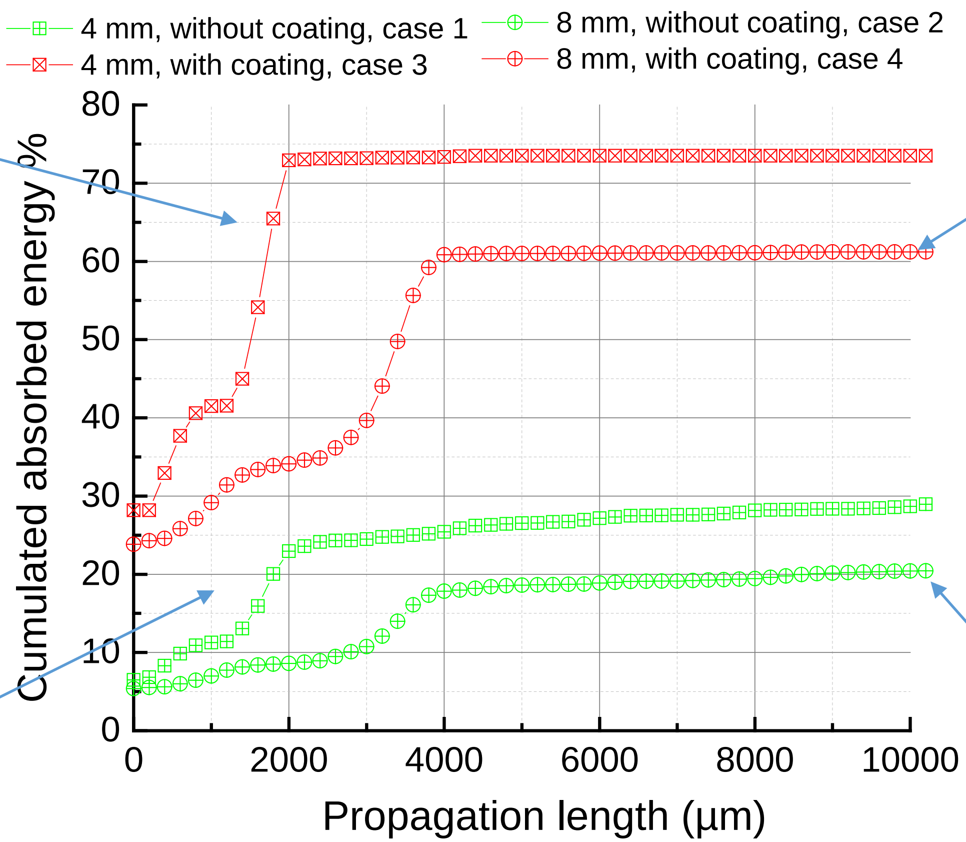

d_{nom}=0,008 m
with coating
case 4

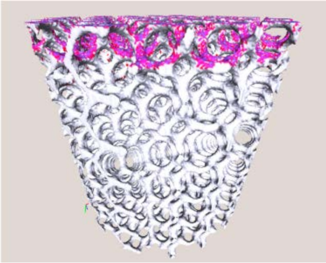

d_{nom}=0,008 m
without coating
case 2

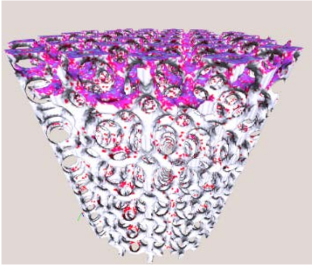

Impact d_{nom} on the absorption of the incident radiative flux and the position of T_{max}

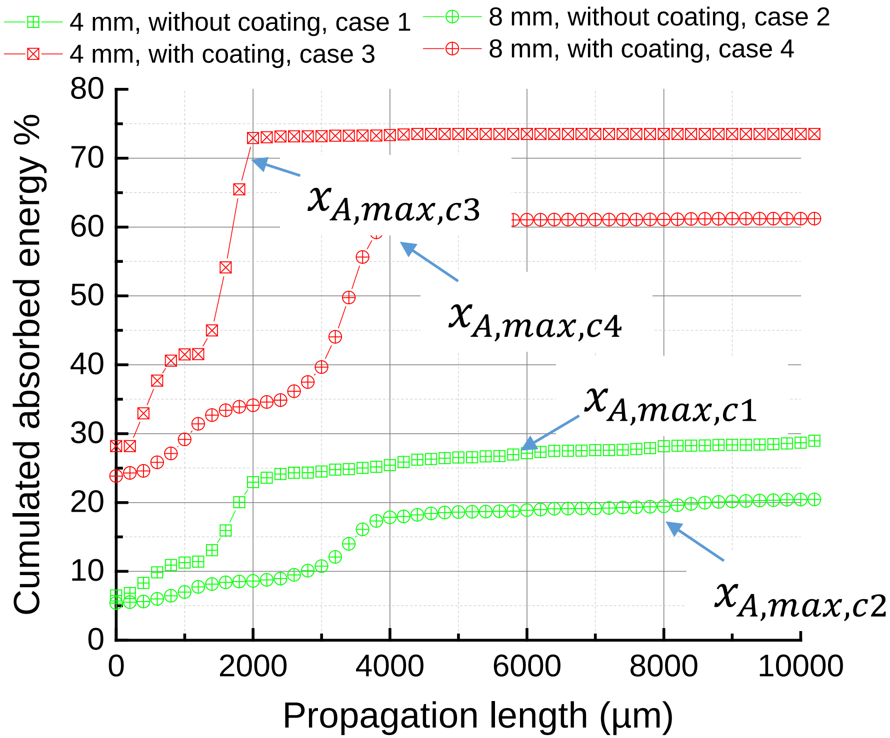

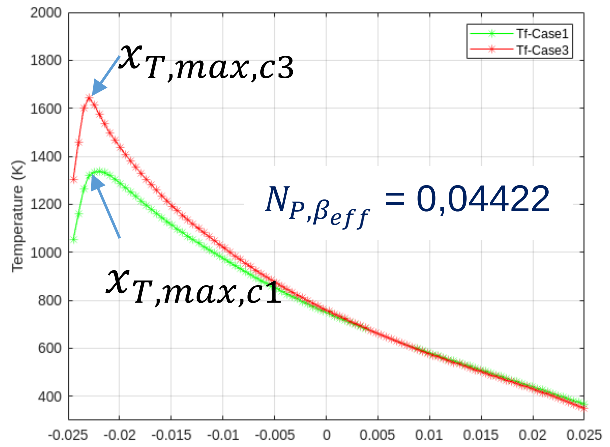

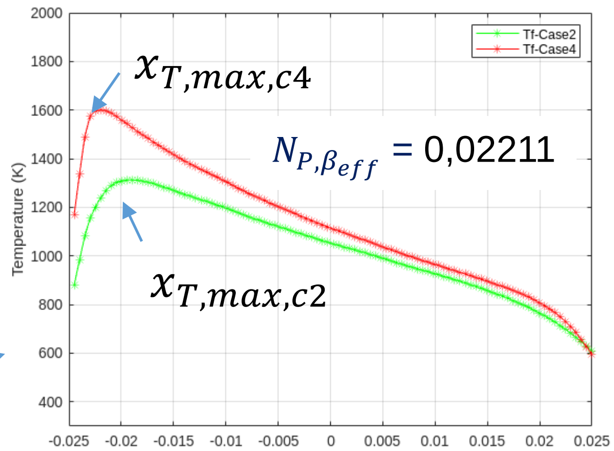

Similar effect

Radiation transport is stopped at the first rank of cell : after conductive (convective) heat transfer

Solar-to-heat performances : OPTISOL bench

PROMES

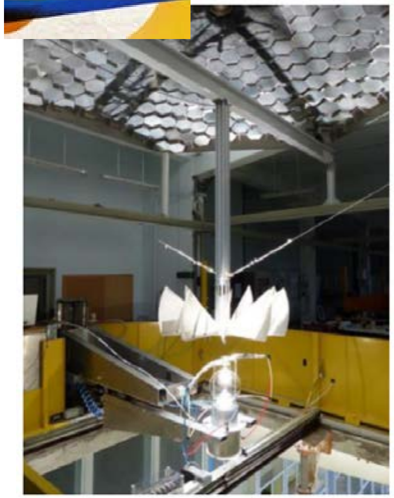

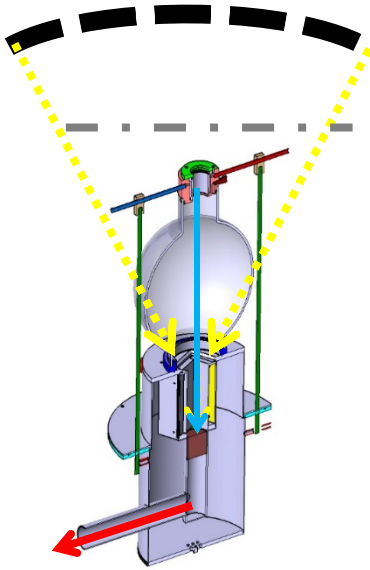

Mey-Cloutier et al., Solar Energy 136 (2016) 226–235

Qualitative agreement but some experiments must still be explained

$$\eta_{ST,1} < \eta_{ST,2} \leftrightarrow N_{P,\beta_{eff},1} > N_{P,\beta_{eff},2}$$

$$\eta_{ST,4} < \eta_{ST,3} \text{ but } N_{P,\beta_{eff},3} > N_{P,\beta_{eff},4}$$

$$\eta_{ST,4} < \eta_{ST,3} \leftrightarrow \omega_{eff,3} < \omega_{eff,4}$$

Modification of the front face for case 4 ?
Heat exchange coefficient?

DNI (W/m²)	q air (g/s)	T out (° C)	η_{ST}
d_{nom}=0,004 m without coating : case 1			
1017	3	219	0,39
1020	2	270	0,33
1022	1	387	0,24
d_{nom}=0,004 m with coating : case 3			
1014	3	423	0,82
1024	2	574	0,75
1014	1	838	0,57
d_{nom}=0,008 m without coating : case 2			
1027	3	307	0,56
1028	2	368	0,46
1024	1	490	0,32
d_{nom}=0,008 m with coating : case 4			
1022	3	382	0,72
1034	2	507	0,64
1034	1	731	0,48

Experimental data

Case 1: $N_{P,\beta_{eff}}$ = 0,04422, ω_{eff} = 0.67

Case 3: $N_{P,\beta_{eff}}$ = 0,04422, ω_{eff} = 0.27

Case 2: $N_{P,\beta_{eff}}$ = 0,02211, ω_{eff} = 0.76

Case 4: $N_{P,\beta_{eff}}$ = 0,02211, ω_{eff} = 0.39

Conduction-to-radiation number

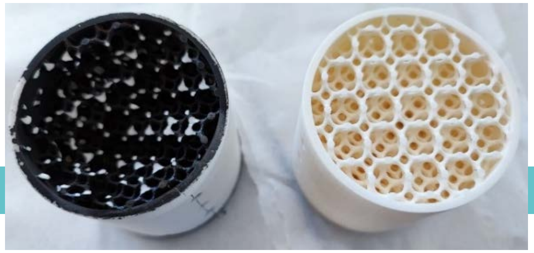

Conclusions & outlook

- Fast and robust FEM solver for conduction-radiation heat exchange modelling through HEM and DS method
- Validation of HEM-DS ↔ Viskanta model (hot and black wall) for a porous structure with a regular lattice (cubic cells)
- Volume propagation of radiation locally increases T→ interest for developing VSR
- Numerical design and elaboration of 4 based-alumina VSR (∅ = 5 cm, h= 5 cm) with stereolitography
- Performance tests with the OPTISOL bench
- Best VSR : porosity 91 %, nominal pore diameter 4 mm with a coating of high solar absorptance
- Planck number not sufficient for following volume propagation within VSR : need to introduce a trapping effect number.

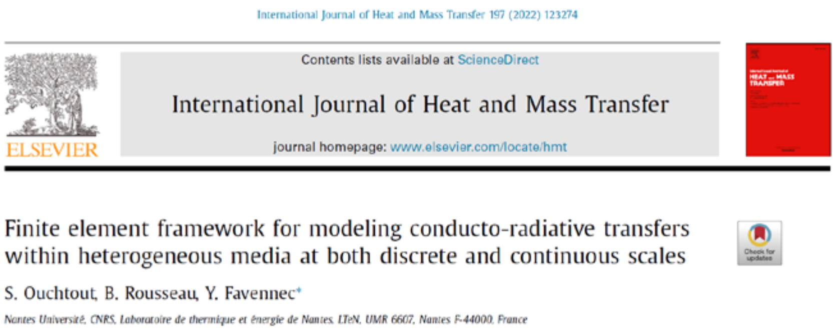
International Journal of Heat and Mass Transfer 197 (2022) 123274

Contents lists available at ScienceDirect

International Journal of Heat and Mass Transfer

journal homepage: www.elsevier.com/locate/hmt

Finite element framework for modeling conducto-radiative transfers within heterogeneous media at both discrete and continuous scales

S. Ouchtout, B. Rousseau, Y. Favennec*

Nantes Université, CNRS, Laboratoire de thermique et énergie de Nantes, LTeN, UMR 6607, Nantes F-44000, France

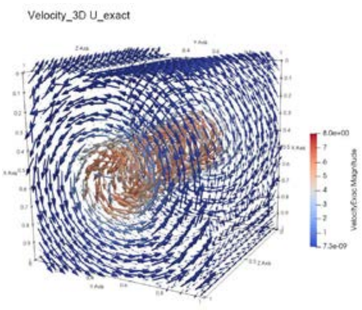

- Coupling with fluid transport (Darcy-Forchheimer - HEM/ Navier-Stokes - DS) → ANCRE SdBE FATHERCASE program (2022-2023) with IFPEN and GeM

- PRC ANR ORCHESTRA (2022-2026) with LTeN-GeM-IFPEN-IRCER
- Topology optimization →
- Thermal shock resistance modelling
- Elaboration of SiC lattice with binder jetting…

Thank you for your attention !

benoit.rousseau@univ-nantes.fr

Influence of the anisotropy factor

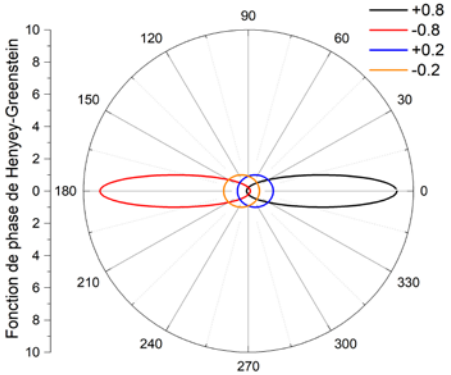

$$P(\widehat{\Omega}' \to \widehat{\Omega}) = \frac{1}{4\pi}\frac{1-g^2}{\left(1+g^2-\widehat{\Omega}.\widehat{\Omega}'\right)^{3/2}}$$

Key quantities

κ_a κ_s

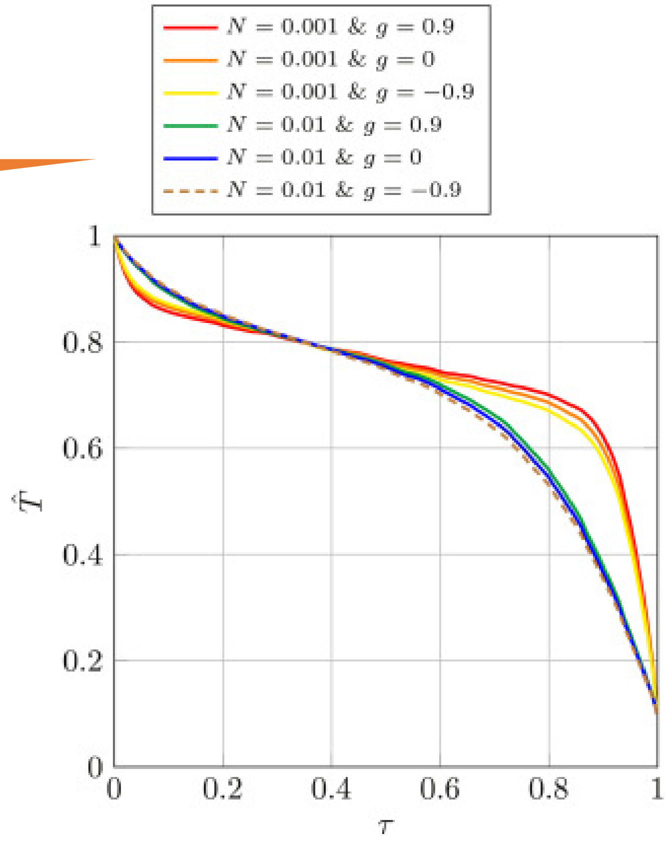

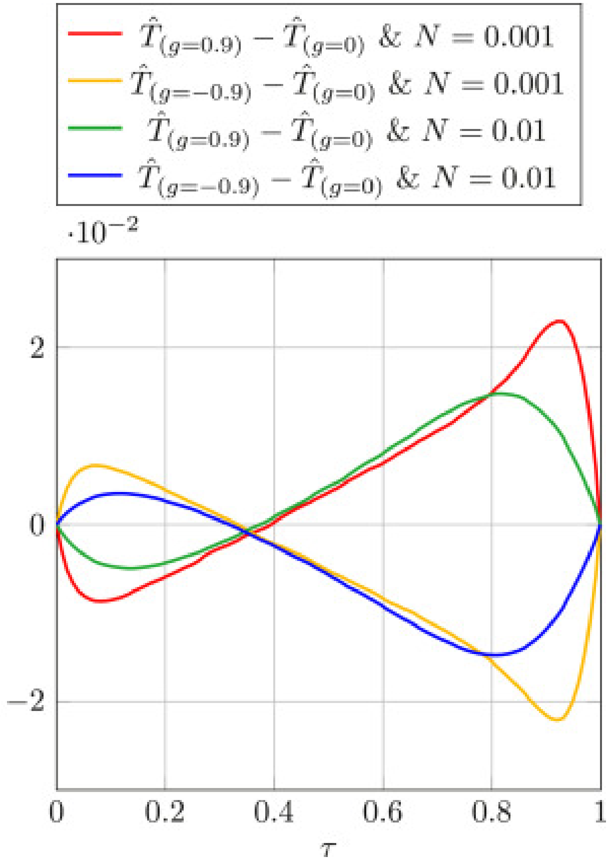

From macro-scale to meso-scale

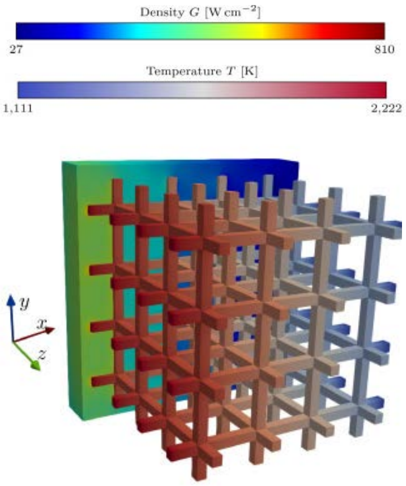

macro → meso

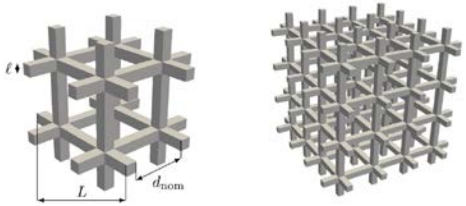

$$p(\ell) = \frac{L^3 - 12\ell^2 L + 16\ell^3}{L^3}; \quad d(\ell) = \frac{L - 2\ell}{2}$$

$$k_{cond,s} = 3\frac{k_{cond,eff}}{1-p}$$

$$\varepsilon_s = 1 - \frac{1-\varepsilon_{eff}}{1-\frac{4}{5}p}$$

S. Guévelou et al., Journal of Quantitative Spectroscopy and Radiative Transfer, 2017, 189, 329-338

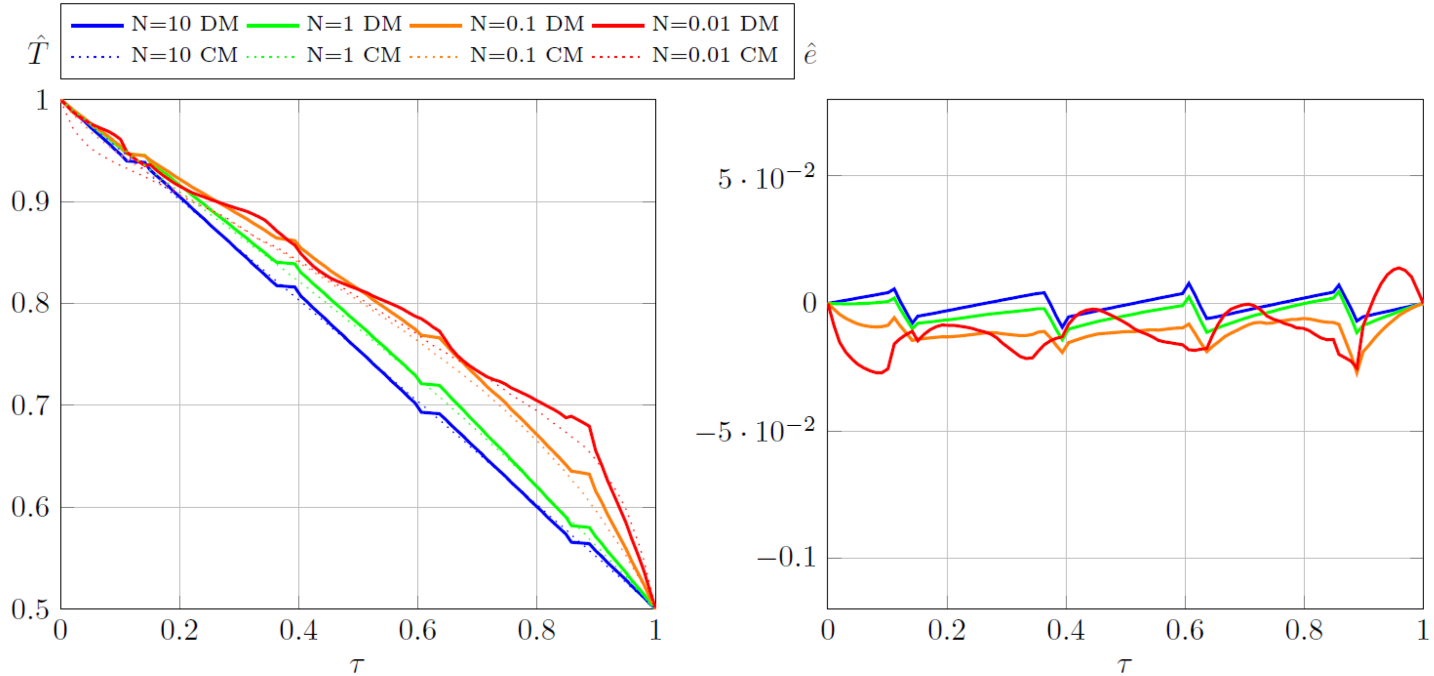

Influence of the albedo